Journal of
Materials Chemistry A

Accepted Manuscript

This article can be cited before page numbers have been issued, to do this please use: W. Yang, H. Zhang, Z. Wang, X. Chu, Z. Xu, H. Su, C. Yan, F. Liu, B. Gu, H. Huang, D. Xiong, H. Zhang and W. Deng, *J. Mater. Chem. A*, 2019, DOI: 10.1039/C9TA01028A.

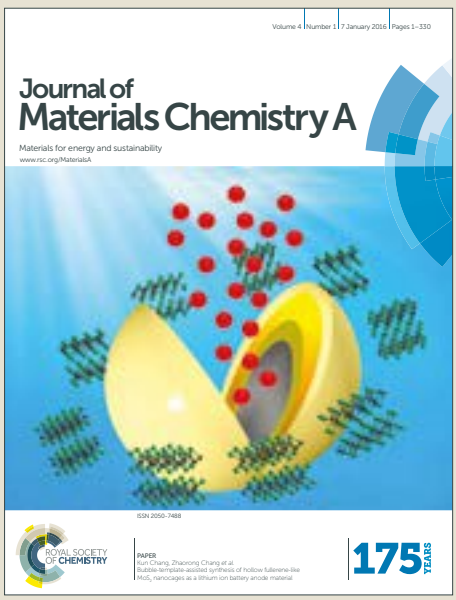

ROYAL SOCIETY OF CHEMISTRY

rsc.li/materials-a

View Article Online
DOI: 10.1039/C9TA01028A

Journal Name

ARTICLE

Extremely low self-discharge solid-state supercapacitor via confinement effect of ion transfer

Received 00th January 20xx,
Accepted 00th January 20xx

DOI: 10.1039/x0xx00000x

www.rsc.org/

Zixing Wang[a], Xiang Chu[a], Zhong Xu[a], Hai Su[c], Cheng Yan[a], Fangyan Liu[a], Bingni Gu[a], Haichao Huang[a], Da Xiong[a], Hepeng Zhang[a], Weili Deng[a], Haitao Zhang[*, a], Weiqing Yang[*, a,b]

Except for low energy density, rapid self-discharge phenomenon also severely limits supercapacitors' application in periodic energy storage and power supply. Herein, we proposed a novel 'playing mud pies' strategy to prepare the high-performance bentonite clay@ionic liquid based solid-state electrolyte (BISE), which can efficiently solve the self-discharge issue of supercapacitors. The BISE-based supercapacitors display extremely low self-discharge behavior with an open circuit potential drop of only 28.9% within 60 h, much better than that of conventional supercapacitors (40.1% @ 12 h). More importantly, even at high temperature of 75 °C, the supercapacitors can still present a low voltage decline of 40% within 12 h and can stably deliver a high voltage of >1.5 V, which guarantees high-temperature energy conversion and storage application. We further proved that the low self-discharge mechanism originates from confinement effect of silicon-oxygen bonds of the clay, which suppress the shuttle effect of Fe ions and promote selective penetration of electrolyte anions. Consequently, the remarkable decrease of both ohmic leakage and diffusion-controlled faradaic process could sharply weaken the self-discharge behavior. Based on BISE, we also developed soft-packaged supercapacitors with a low self-discharge value of 23.6%@20 h. Evidently, our 'playing mud pies' method can open a way to exploit extremely low self-discharge supercapacitors at widely ranging temperatures for deep insight into self-discharge mechanism and further for efficient energy storage of supercapacitors.

Introduction

There is a growing demand for mobile and wireless electronics, so efficient storage of renewable energy becomes a key component.[1-3] As a new type of energy storage device between the battery and traditional capacitor, supercapacitors possess the advantages of long cycle life, fast charging and discharging, environment friendliness, high power density and high safety.[4-6] However, supercapacitors have the disadvantages of low energy density and high self-discharge rate, which limit their widely commercial applications.[7-11] So far, many efforts have been made to study how to improve the capacitance, energy density and power density of supercapacitors, but much less attention has been paid to the general self-discharge phenomenon. Such self-discharge phenomenon will seriously restrict their capacity, energy density and other properties.[1] Therefore, it is mandatory to understand the self-discharge mechanism of supercapacitors better and to suppress the self-discharge phenomenon masterly, which will enable supercapacitors to store energy more efficiently.

As we know, self-discharge is the spontaneous decrease of the voltage for the charged supercapacitors with time on the open circuit. When the supercapacitors are charged, they are in a higher free energy state compared to the discharged state. Therefore, if there are some self-discharge mechanisms, a 'driving force' corresponding to free energy of the discharge tends to reduce the charge spontaneously.[12-15] In general, the main contributions to the self-discharge of the supercapacitors can be summarized into three processes: faradaic reactions with either activation-controlled or diffusion-controlled mechanism,[7, 8, 12, 15] ohmic leakage,[8, 12, 14, 16] and charge redistribution.[16-21] Faradaic reactions include the side reactions caused by the overcharged decomposition of the electrolyte and the redox-reactions caused by impurities or functional groups on the electrodes surface.[12, 14] Ohmic leakage refers to the internal ohmic leakage pathways formed due to the incomplete sealing of bipolar electrodes or inter-electrodes contacts, which leads to self-discharge through the 'Galvanic couple' effect.[8, 12, 14] Charge redistribution related to the concentration gradient is caused by the movement or loss of charge ions adsorbed on the electrode.[16-18] However, there are different self-discharge mechanisms for different systems. So, each self-discharge system should be studied according to specific self-discharge mechanism or any given combination.

[a] Key Laboratory of Advanced Technologies of Materials (Ministry of Education), School of Materials Science and Engineering, Southwest Jiaotong University, Chengdu 610031, PR China.
[b] State Key Laboratory of Traction Power, Southwest Jiaotong University, Chengdu 610031, PR China.
[c] School of Materials Science and Engineering, Key Laboratory of Advanced Ceramics and Machining Technology (Ministry of Education), Tianjin Key Laboratory of Composite and Functional Materials and Tianjin Key Laboratory of Molecular Optoelectronic Science, Tianjin University, Tianjin 300072, PR China
* Correspondence should be addressed to W. Yang (e-mail: wqyang@swjtu.edu.cn) or H. Zhang (e-mail: haitaozhang@swjtu.edu.cn).
Electronic Supplementary Information (ESI) available: [details of any supplementary information available should be included here]. See DOI: 10.1039/x0xx00000x

DOI: 10.1039/C9TA01028A

According to the above self-discharge mechanisms, some breakthroughs had been made in suppressing the self-discharge by adding additives, modifying electrodes, as well as using ion exchange membranes. For examples, Xia et al. proposed electrorheological (ER) effect to suppress the self-discharge.[22] They found that with electrorheological molecules 4-n-pentyl-4'-cyanobiphenyl in the electrolyte, the supercapacitors showed a smaller leakage current of 2.2 μA and it took 13.5 h to drop from 2 V to 1.5 V. Zhang et al. demonstrated the effects of surface chemistry on self-discharge by interfering in the electrostatic interaction between electrolytic ions and the single-walled carbon nanotube and also explored the tunability of the self-discharge process.[23] Lee et al. used the cation exchange membrane instead of a porous separator to prevent redox ion shuttling through the separator.[24] Although the self-discharge of supercapacitors is somewhat alleviated through the above-mentioned strategies, it is still far behind of state-of-the-art, especially at high-temperature conditions.

Here, we proposed a novel strategy to solve the self-discharge issue of supercapacitors using the 'playing mud pies' that is based on bentonite clay cross-linked with ionic liquid through silicon-oxygen bonds and thermoplastic polyurethane to endow mechanical flexibility. The confinement effect of silicon-oxygen bonds in the bentonite clay suppresses the shuttle effect of Fe ions and promotes selectively penetration of electrolyte anions. Consequently, the ratio of self-discharge induced by the ohmic leakage and diffusion-controlled faradaic process declines sharply. Hence, the self-discharge rate of BISE-based supercapacitors is only 28.9% within 60 h, which is an extremely low value compared to that of previously reported work. Moreover, BISE-based supercapacitors also show a low self-discharge rate at high temperature of 75 °C, and BISE can be extended to prepare soft-packaged supercapacitors. Therefore, this work proposed 'playing mud pies' to prepare the extremely low self-discharge supercapacitors that can be applied to periodic energy storage/power supply, even in extreme environments.

Experimental

Preparation of the bentonite clay@ionic liquid based solid-state electrolyte

The bentonite clay@ionic liquid based solid-state electrolyte was fabricated following four steps, named as "playing mud pies". Firstly, the mixtures of bentonite clay and thermoplastic polyurethane (Aladdin Industrial Corporation, Shanghai, China) were obtained by a simply mechanical-blending. During blending, N, N-Dimethylformamide (Kelong Chemical Reagent Corporation, Chengdu, China) was used as the solvent. Then, the mixture was pressed into a film of 0.15 mm thick by a roller machine. After the film was punched into small discs with a diameter of 16 mm or an area of 6 cm^2, the discs were dried at 100 °C for 24 h. Finally, the freestanding films were transferred to the glove box (MBraun Unilab Plus) and immersed into the 1-Ethyl-3-methylimidazolium Tetrafluoroborate ($EMIMBF_4$, Aladdin Industrial Corporation, Shanghai, China) ionic liquid to form a solid-state electrolyte, named as BISE.

Microstructural and composition characterizations

Field-emission scanning electron microscopy (FESEM) was carried out on FEI QUANTA FEG 250. Thermogravimetry (TG) analysis was carried out with NETZSCH STA449F3. Contact-angle was measured using Dataphysics DSA100 contact-angle system. Brunauer-Emmett-Teller (BET) surface areas and density functional theory (DFT) pore size distribution measurements of activated carbon (AC) and hierarchical carbon tubular nanostructures (*h*CTNs)[25,26] were performed with Micromeritics ASAP 2020 surface area and pore size analyzer using N_2 adsorption/desorption isotherm at -196 °C.

Electrochemical measurements

The activated carbon (AC, YP-50F) electrodes coated on aluminum foil are constructed with 85:8:1:6 wt% of the AC, Super C45 (conductive agent), carboxymethyl cellulose and styrene butadiene rubber (binder). The electrode possesses ~200 μm in thickness. The hierarchical carbon tubular nanostructures (*h*CTNs) electrodes were synthesized on stainless steel meshes (500 meshes) substrate by a simple method of Mg reaction with CO_2 gas. The electrode possesses 12 mm in diameter. The ionic liquid was 1-ethyl-3-methylimidazolium tetrafluoroborate ($EMIMBF_4$). Supercapacitors were assembled using 2032 coin cells in an argon-filled glovebox with oxygen and water below 0.1 ppm. The soft-packaged supercapacitors were sandwiched into two symmetrical AC electrodes and a solid-state electrolyte. The electrodes were welded to the electrode lugs by the ultrasonic spot welder, placed in an aluminum plastic bag, and then vacuum dried at 85 °C for 24 h. Finally, the vacuum pre-sealing machine sealed the aluminum plastic bag.

The cyclic voltammetry (CV) curves, galvanostatic charge-discharge (GCD) process and electrochemical impedance spectroscopy (EIS) were carried out using the electrochemical workstation (CHI660E). The self-discharge tests of the supercapacitors were measured on an Arbin MSTAT4 multi-channel galvanostat/potentiostat instrument.

Results and discussion

Bentonite clay@ionic liquid based solid-state electrolyte

The conventional supercapacitors using the liquid electrolytes and porous polymer separators possess severe self-discharge problem (Fig. 1a). On the one hand, the fast movement of electrolyte ions leads to rapid potential decay because of gradient concentration of electrolyte ions. On the other hand, the limited mechanical strength of the polymer membrane brings into Ohmic leakage passage for the electrons. Hence, replacing both the liquid electrolytes and the polymer separators by solid-state electrolytes for novel supercapacitors probably solve the old issue of self-discharge (Fig. 1a). A simple

View Article Online
DOI: 10.1039/C9TA00103A

and effective 'playing mud pies' method was utilized to produce freestanding solid-state films that were composed of bentonite clay, $EMIMBF_4$ ionic liquid and thermoplastic polyurethane, called BISE (Fig. 1b). The bentonite clay in the BISE shows a layered structure (Electronic Supplementary Information, ESI, Fig. S1) and possess abundant of Si-O bonds. The latter gifts surface negative charges of the BISE and hence can interact with $EMIM^+$ ions (Fig.1b and ESI Fig. S2). Consequently, $EMIM^+$ cations can replace small cations like H^+ and locate at the interlamination of the bentonite clay, as indicated by the previously reported works.[27-30] From the results of the EDS (ESI Fig. S3), we further verified that $EMIMBF_4$ ionic liquid could be well combined with bentonite clay. To estimate the ionic liquid uptake, we immersed the freestanding films made from the mixtures of bentonite clay and thermoplastic polyurethane into $EMIMBF_4$. After 1 h, the total absorption of the ionic liquid was 39.4 (± 2.3) wt%, which was determined by high precision electronic balance (MS105DU). In addition, the bentonite clay-based film has a good affinity for ionic liquids determined from the contact angle test (ESI Fig. S4).

TG (Fig. 1c) and DSC curves (ESI Fig. S5) demonstrate that the BISE and its components exhibit good thermal stability within 250 °C, which ensures that it can be a multifunctional film in a variety of high temperature energy conversion and storage application. Besides thermal stability, the ionic conductivity of solid-state electrolytes has always been a concern. Here we determined its value using electrochemical impedance plots (ESI, Fig. S6). Fig. 1d and Fig. S7 show the Nyquist plots with frequency ranging from 10^{-2} to 10^6 Hz at different temperatures. With fitted by Z-view using the equivalent circuit (Fig. 1d and ESI, Fig. S7), where R_0, R_{ct}, CPE1, W_0 represent the resistance of the electrolyte, charge transfer resistance, electric double layer capacitance, Warburg impedance, respectively, the ionic conductivities are 2.1×10^{-4} S m^{-1} at 25 °C, 4.4×10^{-4} S m^{-1} at 50 °C, 8.1×10^{-4} S m^{-1} at 75 °C and 1.9×10^{-3} S m^{-1} at 100 °C, respectively, which are close to other reported all solid-state electrolytes.[31, 32] Hence, the combined series resistance decreases with increasing temperature and the ionic conductivity of the BISE gradually increases with increasing temperature that is advantage for high-temperature energy storage.

The designed BISE films can be used not only as the electrolyte but also the separator. Hence, all solid-state supercapacitors with activated carbon electrodes and BISE could be assembled. Comparing to conventional supercapacitors using liquid electrolytes, all solid-state supercapacitors with BISE exhibit an extremely low self-discharge as shown in Fig. 1e. Open circuit potential measurement was used to monitor the change of potential with time under open circuit condition. Both the conventional supercapacitors and BISE-based supercapacitors were charged to 3 V at a current density of 0.5 mA cm^{-2} and then recorded the self-discharge. Amazingly, BISE-based supercapacitors show a very low self-discharge rate (final voltage/initial voltage) of only 28.9% after 60 h (Fig. 1e). In contrast, the open circuit potential of the conventional supercapacitors with cellulose membrane dropped by 40.1% within a short time of 12 h. It means that the self-discharge rate decreases by ~10% as the shelved time increased by four times for BISE-based supercapacitors. Moreover, during a long period time of record, BISE-based supercapacitors can maintain a voltage above 2 V, which is

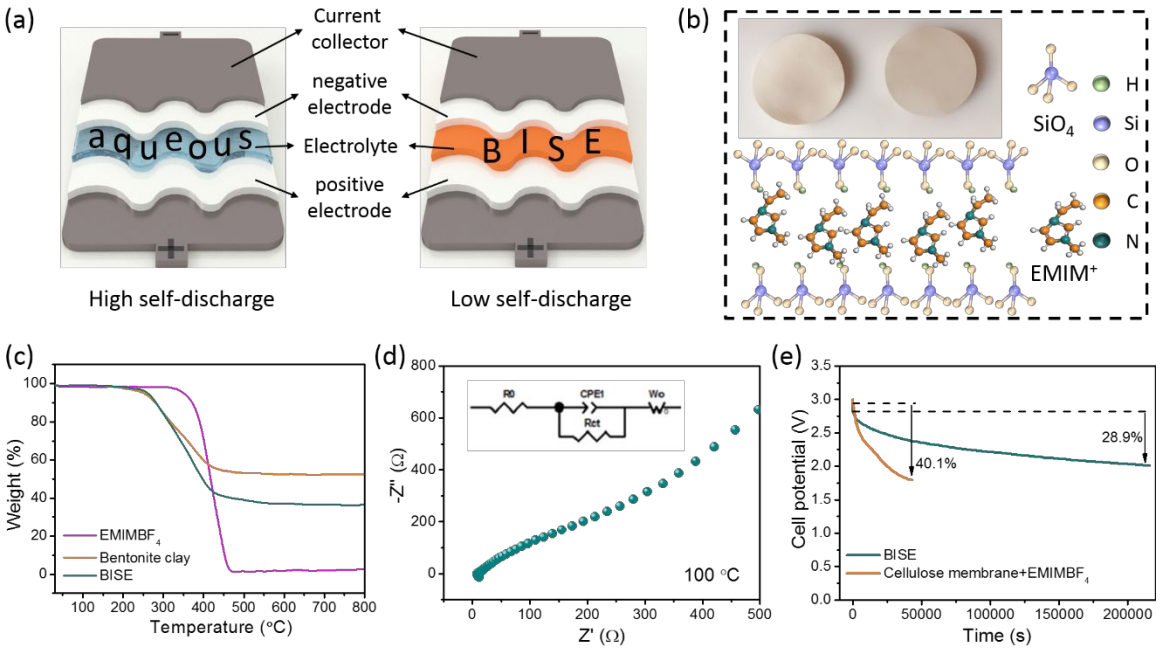

Figure 1. The strategy to design low self-discharge supercapacitors using BISE solid-state electrolyte. (a) Schematic illustration of the liquid electrolyte and the solid-state BISE electrolyte. (b) Schematically showing the interaction of $EMIM^+$ ions with bentonite clay surface charges, and the top shows the photograph of the solid-state film. (c) TG curves of the $EMIMBF_4$, bentonite clay and the BISE. (d) EIS spectrum at 100 °C and its equivalent circuit. (e) Open circuit potential decays for conventional supercapacitors and BISE solid-state supercapacitors.

View Article Online
DOI: 10.1039/C9TA01028A

higher than the commonly acceptable voltage for powering electronic devices (1.5 V).

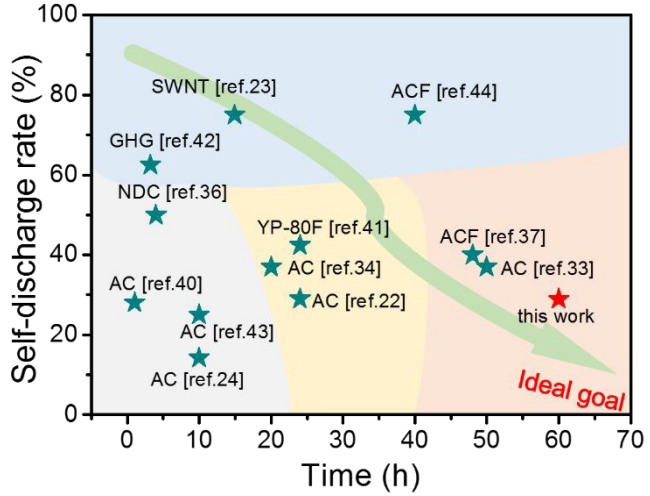

Figure 2. Self-discharge rate comparison of previously reported works. (AC: activated carbon, SWNT: single-walled carbon nanotubes, NDC: N-doped carbon nanosheets, GHG: graphene hydrogel, ACF: activated carbon fiber)

The self-discharge of our BISE-based supercapacitors compares favorably with other reported supercapacitors (Fig. 2 and ESI, Table S1).[22-24, 33-44] Employing BISE did not only reduce the self-discharge but also improve the safety. We anticipated that by implementing a solid-state electrolyte with flexibility and high ionic conductivity, the performance of the supercapacitors would be further improved, making the self-discharge closer to the ideal goal. Consequently, the extremely low self-discharge reduces the significant loss of stored energy, enabling it to supply more sustained energy which may expand the applications of supercapacitors, such as used in periodic energy storage and power supply. Surprisingly, through facile 'playing mud pies' method to make solid-state electrolyte, the novel BISE-based supercapacitors deliver quite lower self-discharge rate than conventional supercapacitors, which stimulate us to disclose the mechanism leading to extremely low self-discharge phenomenon.

Self-discharge mechanism of the BISE-based supercapacitors

In order to better control the self-discharge process, we analyzed the self-discharge mechanism in BISE supercapacitor systems. Fig. 3a shows the decays of open circuit potential after charging with different current densities. As expected, the current density not only has an effect on self-discharge but also on the initial voltage. The initial voltage increases linearly as the current density decreases (the inset of the Fig. 3a). The reason lies that lower current density allows enough time for ions to distribute and hence form a much more stable electric double layer, while the ions stack together quickly to form an unstable electric double layer at a high current density. The change in the cumulative amount of ions within the electric double layer causes the voltage drop at the beginning of the self-discharge process, so the initial voltage at the beginning of the self-

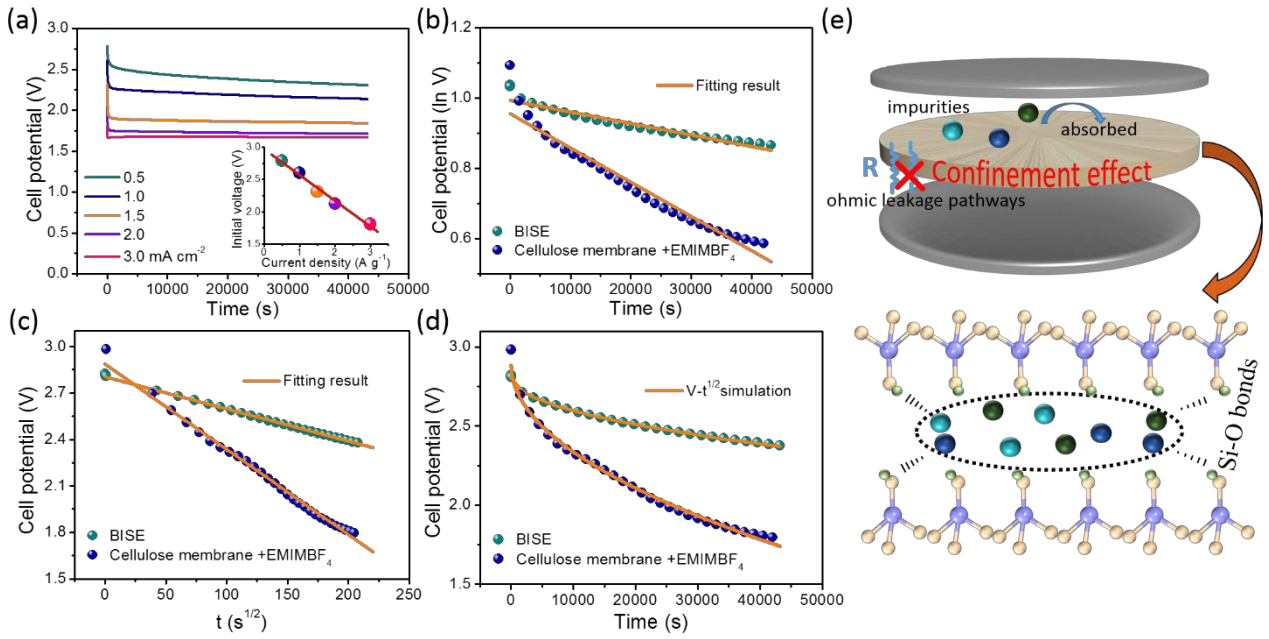

Figure 3. The self-discharge mechanisms of the conventional supercapacitors and the BISE supercapacitors. (a) Open circuit potential decays for the BISE-based supercapacitors after charging with different charge current densities from 0.5 to 2 mA g^{-1}. (b) Fitted curves by the potential driving model. (c) Fitted curves by the diffusion-controlled model. (d) The simulation results by the diffusion-controlled model. (e) Schematically illustrating the suppressed self-discharge phenomenon from confinement effect of BISE via Si-O bonds to absorb the impurities and promote selective penetration of electrolyte anions.

View Article Online
DOI: 10.1039/C9TA01028A

discharge process should replace the nominal voltage (3.0 V) when calculating the self-discharge rate.

Conway et al. proposed three mechanisms to describe the self-discharge, the ohmic leakage, diffusion-controlled faradaic process and activation-controlled faradaic process. For eliminating overcharged beyond the electrolyte/solvent decomposition potential induced activation-controlled faradaic processes, the cell potential was chose to be 3.0 V which was much lower than the nominated voltage of $EMIMBF_4$ ionic liquid electrolyte. As to the self-discharge by ohmic leakage (potential driving model), the characteristic self-discharge behavior of ohmic leakage is modeled as Eq. 1.[8, 12, 16]

$$V = V_0 \exp(-\frac{t}{RC}) \quad (1)$$

Where V is the supercapacitor voltage during the self-discharge, V_0 is the initial potential of the charged supercapacitor (3 V in this work), t is the time and RC corresponds to the time constant of the self-discharge process. According to Eq. 1, the fitted self-discharge curves for both conventional supercapacitors and BISE-based supercapacitors displayed great deviations from the actual curves (Fig. 3b). It can be concluded that the ohmic leakage model is not the main factor to induce self-discharge, which is coincided with the high mechanical strength and large electrical insulation characteristics of the BISE electrolyte.

Taking diffusion-controlled model into account, the self-discharge curves displayed a linear relation between V and $t^{1/2}$ according to Eq. 2.[8, 12, 14]

$$V = V_0 - m\sqrt{t} \quad (2)$$

Where m is the diffusion parameter and represents the diffusion rate of the ions near the electrode surface. Using diffusion-controlled model, the correlation coefficients R^2 are > 0.99 (Fig. 3c). In addition, the two curves can match perfectly, which further proves this linear relation (Fig.3 d). Therefore, the diffusion-controlled faradaic processes cause the self-discharge processes for both conventional supercapacitors and BISE-based supercapacitors. The reasons for extremely low self-discharge BISE-based supercapacitors attribute to the following three aspects. First of all, the prepared BISE possesses a high mechanical strength that can prevent the formation internal short circuit. This effect could be confirmed by the fact that the morphology of BISE (ESI, Fig. S8) did not change before and after self-discharge processes. Secondly, BISE limits the diffusion of impurities via confinement effect of ion transfer. The diffusion-controlled faradaic process commonly refers to some depolarizing impurities (e.g. Fe^{2+}, Fe^{3+}, O_2) caused faradaic reaction within the potential range of charging. As mentioned in M. Sjödin's work[45, 46], due to the kinetically limiting Faradaic reaction of polypyrrole, a reactive intermediate was formed, resulting in self-discharge. The diffusion parameter 'm' of the conventional supercapacitor is 5.52×10^{-3} V $s^{-1/2}$, much larger than the BISE-based supercapacitors (2.09×10^{-3} V $s^{-1/2}$), which indicates that the BISE inhibits the diffusion of impurity ions. As schematically shown in Fig. 3e, small cations between bentonite clay are replaced by impurity ions, which limits the formation of redox shuttles diffuse between the two electrodes. Thirdly, confinement effect of silicon-oxygen bonds of the bentonite clay promotes selective penetration of electrolyte anions which further suppresses the self-discharge. Therefore, this BISE electrolyte can also be applied to hierarchical carbon tubular nanostructures (*h*CTNs) (ESI, Fig. S9) and organic electrolyte (ESI, Fig. S10) due to the extremely low self-discharge.

Effect of temperature on self-discharge process

Self-discharge is a rate process, so the self-discharge rates of supercapacitors at high temperature are generally accelerated, which is based on well-known kinetic effects (Eyring and Arrhenius equations) associated with activation energy.[12, 15, 47] However, the self-discharge rate of BISE-based supercapacitors at high temperatures is much slower probably due to the excellent thermal stability of BISE (Fig. 1c). To investigate the effect of temperature on self-discharge, we tested the self-discharge curve of BISE-based supercapacitors citors at 25 °C, 50 °C and 75 °C (Fig. 4a). It is apparent that the self-discharge process is the slowest at a low temperature (25 °C). However, the open circuit potential of the BISE supercapacitor only drops by about 40% within 12 h at 75 °C, and the voltage can be maintained above 1.5 V, which is a great advantage compared to other devices. In addition, the internal resistance of the device decreases with the increase of temperature while the initial

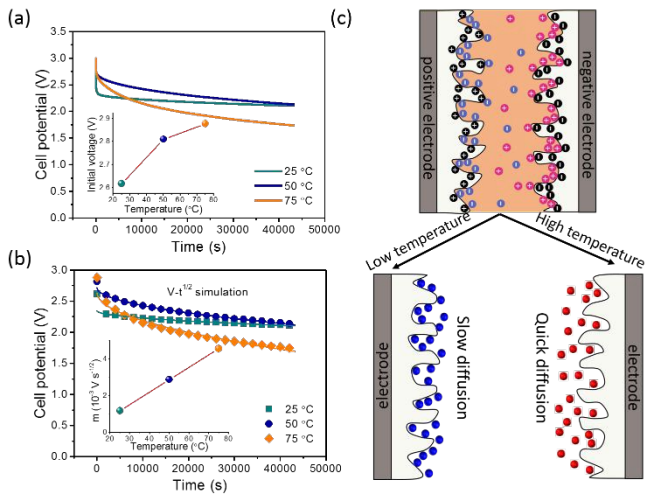

Figure 4. The self-discharge of the BISE supercapacitor at different temperatures. (a) Open circuit potential decays of the BISE-based supercapacitors at 25−75 °C. (b) The fitted results by the diffusion-controlled model. (c) Schematic illustration of the diffusion process at different temperatures.

View Article Online
DOI: 10.1039/C9TA01028A

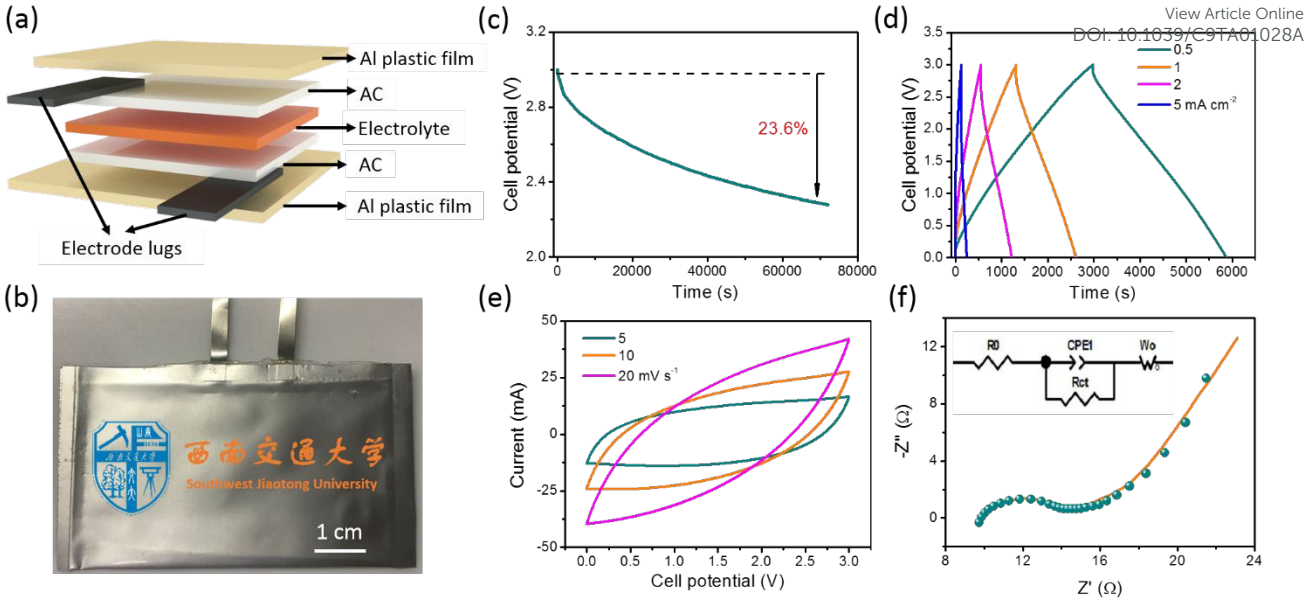

Figure 5. The self-discharge of the soft-packaged supercapacitors. (a) Schematic illustration of the internal structure. (b) Photograph of the soft-packaged supercapacitors. (c) Open circuit potential decay. (d) GCD curves at various current densities from 0.5 to 5 mA cm^{-2}. (e) CV curves at various scan rates from 5 to 20 mV s^{-1}. (f) Nyquist plots, equivalent circuit and the fitted results.

voltage (inset of the Fig. 4a) and capacity increase gradually (ESI, Fig. S11). The specific capacitance of BISE-based supercapacitor can reach 80 F g^{-1} at 25 °C and 100 F g^{-1} at 75 °C, which suggests that the BISE can effectively supress the self-discharge phenomenon without seriously weakening specific capacitance of the supercapacitors.

Furthermore, diffusion-controlled model applied at room temperature is still valid in the wide temperature window of the BISE supercapacitor system, as shown in the Fig. 4b. The diffusion parameters obtained by the fitting method gradually increases with the increase of temperature, and the diffusion parameter reaches 4.55×10^{-3} V s$^{-1/2}$ at 75 °C, which is equivalent to four times of 25 °C. The diffusion parameters at higher temperatures are much larger, which means that the ions diffuse much faster, resulting in much faster charge loss from the electric double layer, which ultimately leads to more serious self-discharge, as illustrated in Fig. 4c. However, the diffusion parameters of BISE supercapacitor at high temperatures are still much lower than most other work, which is still due to the confinement effect of BISE. On the one hand, as the temperature increases, the excellent thermal stability of BISE inhibits the rapid decay of the viscosity; On the other hand, it suppresses the increase of ion activation energy, and thus the ion mobility is severely limited.

Soft-packaged supercapacitors

After addressing the self-discharge issue, we further explore the practical application of BISE supercapacitors. We assembled a soft-packaged supercapacitor (75 × 40 mm) using BISE as shown in Fig. 5a-b. Fig. 5c shows the open circuit potential in 20 h of the soft-packaged supercapacitor after fully charged to 3 V with a current density of 0.5 mA cm^{-2}. It can be clearly observed that after 20 h, the open circuit potential of the soft-packaged supercapacitor only drops to nearly 2.3 V, which is only 23.6% lower than the initial voltage. This extremely low self-discharging soft-packaged supercapacitor can store energy more efficiently and further promote the commercial use of supercapacitors. Cyclic voltammetry (CV) and galvanic charge-discharge (GCD) measurements were performed before the self-discharge test to ensure the stability of the initial voltage. Fig. 5d shows the GCD curves at various current densities from 0.5 to 5 mA cm^{-2}, which shows the symmetrical triangular shape, indicating excellent electrochemical reversibility. Based on the GCD curve with a current density of 0.5 mA cm^{-2}, the calculated capacitance is 37.6 F g^{-1}. The electric double layer capacitive behavior also can be observed from the CV curves (Fig. 5e), which are similar to nearly rectangles. Fig. 5f shows the Nyquist plots of the soft-packaged supercapacitor fitted by Z-view using the equivalent circuit shown in the inset of the Fig. 5f, where the real axis intercept is almost around 10 Ω. However, the charge transfer resistance and ion transfer resistance are relatively large. We anticipated that by adding bentonite clay as the additive to the electrolyte or modifying the electrodes to improve the conductivity, the performance of the supercapacitors would be further improved.

Conclusions

In summary, a novel 'playing mud pies' strategy had been designed to successfully manufacture the high-performance bentonite clay@ionic liquid based solid-state electrolyte. These BISE-based supercapacitors demonstrated an open circuit potential decline of only 28.9% and maintain a voltage above 2 V after 60 h. Even at high temperature of 75 °C, the

supercapacitors could also present a low voltage decline of 40% within 12 h and could stably deliver a high voltage of >1.5 V. From the perspective of electrolytes, the confinement effect of silicon-oxygen bonds in the bentonite clay declines the ohmic leakage and diffusion-controlled faradaic process. Based on BISE, the as-developed soft-packaged supercapacitors remarkably presented a low self-discharge value of 23.6%@20 h. Evidently, this 'playing mud pies' method will open a way to probe the mechanism of self-discharge and provide a new concept for the expanded exploitation of low self-discharge supercapacitors with high energy storage.

Conflicts of interest

There are no conflicts to declare.

Acknowledgements

We are thankful to Southwest Jiaotong University Analytical and Testing Center for the SEM measurements. This work is supported by the National Natural Science Foundation of China (No. 51602265), the Special Funding of China Postdoctoral Science Foundation (No. 2018T110992), the Sichuan Science and Technology Program (No. 2018RZ0074) as well as the Cultivation Program for the Excellent Doctoral Dissertation of Southwest Jiaotong University (No. D-YB201709).

Notes and references

1 Y. Shao, M. F. El-Kady, J. Sun, Y. Li, Q. Zhang, M. Zhu, H. Wang, B. Dunn and R. B. Kaner, *Chem. Rev.*, 2018, **118**, 9233-9280.
2 Y. Wang, Y. Song and Y. Xia, *Chem. Soc. Rev.*, 2016, **45**, 5925-5950.
3 J. Q. Liu, M. B. Zheng, X. Q. Shi, H. B. Zeng and H. Xia, *Adv. Funct. Mater.*, 2016, **26,** 919-930.
4 H. Huang, H. Su, H. Zhang, L. Xu, X. Chu, C. Hu, H. Liu, N. Chen, F. Liu, W. Deng, B. Gu, H. Zhang and W. Yang, *Adv. Electron. Mater.*, 2018, **4**, 1800179.
5 N. Jabeen, A. Hussain, Q. Y. Xia, S. Sun, J. W. Zhu and H. Xia, *Adv. Mater.*, 2017, **29,** 1700804.
6 X. Chu, H. Zhang, H. Su, F. Liu, B. Gu, H. Huang, H. Zhang, W. Deng, X. Zheng and W. Yang, *Chem. Eng. J.*, 2018, **349**, 168-175.
7 I. S. Ike, I. Sigalas and S. Iyuke, *Phys. Chem. Chem. Phys.*, 2016, **18**, 661-680.
8 H. A. Andreas, *J. Electrochem. Soc.*, 2015, **162**, A5047-A5053.
9 J. Niu, B. E. Conway and W. G. Pell, *J. Power Sources*, 2004, **135**, 332-343.
10 A. Lewandowski, P. Jakobczyk, M. Galinski and M. Biegun, *Phys. Chem. Chem. Phys.*, 2013, **15**, 8692-8699.
11 S.-E. Chun, B. Evanko, X. Wang, D. Vonlanthen, X. Ji, G.D. Srucky and S. W. Boettcher, *Nat. Commun.*, 2015, **6**, 7818.
12 B. E. Conway, W. G. Pell and T.-C. Liu, *J. Power Sources*, 1997, **65**, 53-59.
13 W. G. Pell, B. E. Conway, W. A. Adams and J. Oloveora, *J. Power Sources*, 1999, **80**, 134-141.
14 T. Liu, W. G. Pell and B. E. Conway, *Electrochim. Acta*, 1997, **42**, 3541-3552.
15 B. W. Ricketts and C. T.-That, *J. Power Sources*, 2000, **89**, 64-69.
16 J. Black and H. A. Andreas, *Electrochim. Acta*, 2009, **54**, 3568-3574.
17 M. A. Davis and H. A. Andreas, *Carbon*, 2018, **139**, 299-308.
18 J. Black and H. A. Andreas, *J. Power Sources*, 2010, **195**, 929-935.
19 C. Hao, X. Wang, Y. Yin and Z. You, *J. Electron. Mater.*, 2016, **45**, 2160-2171.
20 M. Kaus, J. Kowal and D. U. Sauer, *Electrochimi. Acta*, 2010, **55**, 7516-7523.
21 J.-F. Shen, Y.-J. He and Z.-F. Ma, *J. Power Sources*, 2016, **303**, 294-304.
22 M. Xia, J. Nie, Z. Zhang, X. Lu and Z. L. Wang, *Nano Energy*, 2018, **47**, 43-50.
23 Q. Zhang, C. Cai, J. Qin and B. Wei, *Nano Energy*, 2014, **4**, 14-22.
24 J. Lee, A. Tolosa, B. Krüner, N. Jäckel, S. Fleischmann, M. Zeiger, D. Kim and V. Presser, *Sustain. Energ. Fuels*, 2017, **1**, 299-307.
25 H. Su, H. Zhang, F. Liu, F. Chun, B. Zhang, X. Chu, H. Huang, W. Deng, B. Gu, H. Zhang, X. Zheng, M. Zhu and W. Yang, *Chem. Eng. J.*, 2017, **322**, 73-81.
26 H. Zhang, H. Su, L. Zhang, F. Chun, X. Chu, W. He and W. Yang, *J. Power Sources*, 2016, **331**, 332-339.
27 J. U. Ha and M. Xanthos, *Green Chem. Lett. Rev.*, 2011, **4**, 103-107.
28 H. Hu, J. C. Martin, M. Zhang, C. S. Southworth, M. Xiao, Y. Meng and L. Sun, *RSC Adv.*, 2012, **2**, 3810.
29 A. Pucci, V. Liuzzo, B. Melai, C. S. Pomelli and C. Chiappe, *Polym. Int.*, 2012, **61**, 426-433.
30 P. Sivaraman, K. Shashidhara, A. P. Thakur, A. B. Samui and A. R. Bhattacharyya, *Polym. Eng. Sci.*, 2015, **55**, 1536-1545.
31 H. Xie, J. B. Goodenough and Y. Li, *J.Power Sources*, 2011, **196**, 7760-7762.
32 G. Y. Adachi, N. Imanaka and H. Aono, *Adv. Mater.*, 1996, **8**, 127-135.
33 E. Mourad, L. Coustan, P. Lannelongue, D. Zigah, A. Mehdi, A. Vioux, S. A. Freunberger, F. Favier and O. Fontaine, *Nat. Mater.*, 2017, **16**, 446-453.
34 K. Fic, G. Lota and E. Frackowiak, *Electrochimi. Acta*, 2010, **55**, 7484-7488.
35 F. Soavi, C. Arbizzani and M. Mastragostino, *J. Appl. Electrochem.*, 2013, **44**, 491-496.
36 T. Xiong, Z. G. Yu, W. S. V. Lee and J. Xue, *ChemSusChem*, 2018, **11**, 3307-3314.
37 Q. Zhang, J. Rong, D. Ma and B. Wei, *Energ. Environ. Sci.*, 2011, **4**, 2152-2159.
38 T. Sato, S. Marukane, T. Morinaga, T. Kamijo, H. Arafune and Y. Tsujii, *J. Power Sources*, 2015, **295**, 108-116.
39 J. Wang, B. Ding, X. Hao, Y. Xu, Y. Wang, L. Shen, H. Dou and X. Zhang, *Carbon*, 2016, **102**, 255-261.
40 T. Tevi, H. Yaghoubi, J. Wang and A. Takshi, *J. Power Sources*, 2013, **241**, 589-596.
41 A. Laheäär, A. Arenillas and F. Béguin, *J. Power Sources*, 2018, **396**, 220-229.
42 L. Chen, H. Bai, Z. Huang and L. Li, *Energ. Environ. Sci.*, 2014, **7**, 1750-1759.
43 J. Lee, S. Choudhury, D. Weingarth, D. Kim and V. Presser, *ACS Appl. Mater. Inter.*, 2016, **8**, 23676-23687.
44 S. Nohara, H. Wada, N. Furukawa, H. Inoue and C. Iwakura, *Res. Chem. Intermediat.*, 2006, **32**, 491-496.
45 H. Olsson, E. J. Berg, M. Strømme and M. Sjödin, *Elctrochem. Commun.*, 2015, **50**, 43-46.
46 H. Olsson, Z. Qiu, M. Strømme and M. Sjödin, *Phys. Chem. Chem. Phys.*, 2015, **17**, 11014-11019
47 H. Yang and Y. Zhang, *J. Power Sources*, 2011, **196**, 8866-8873.

View Article Online
DOI: 10.1039/C9TA01028A

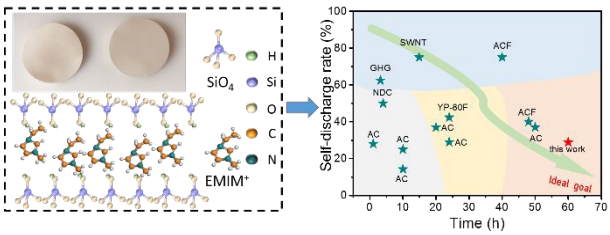

The bentonite clay@ionic liquid based solid-state electrolyte can effectively suppress the self-discharge rate via confinement effect of ion transfer.